

CHARACTERIZATION OF CHITOSAN FROM *RHYNCHOPHORUS PHOENICIS* AND SYNTHESIS OF ITS ALUMINA NANOCOMPOSITE

*Osu, C. I., Ugwu, H. C., and Iwuoha, G. N.

Department of Pure and Industrial Chemistry, Faculty of Science, University of Port Harcourt, Port Harcourt.
 charsike@yahoo.com

Received: 06-10-2021

Accepted: 10-11-2021

ABSTRACT

Rhynchophorus phoenicis, found in the tropical regions of Africa where it is regarded as a pest was used to synthesize chitosan and alumina-chitosan nano-composite. The synthesized Chitosan and alumina-chitosan nano-composite were characterized using instrumental methods of analysis which include Fourier Transform Infrared Spectroscopy (FTIR), X-ray Diffraction (XRD), Scanning Electron Microscope (SEM). FTIR reveals the existence of OH stretching vibration –NH stretching, NH bonding, vibration of methylene C-H bonding, O=C=O stretching, C-N bonding stretching and CO stretching vibration at 3842.33 cm⁻¹, 3402.54 cm⁻¹, 3286.81 cm⁻¹, 2939.61 cm⁻¹, 1527.67 cm⁻¹, 1303.92 cm⁻¹ and 1041.60 cm⁻¹ respectively. The scanning electron micrograph proves that the chitosan has large particles that are regular with paltry pores while alumina-chitosan nano-composite has fairly small particles and porous surface with significant pores. X-ray diffractogram showed a distinct stretch at 22°; 16° and 25°; 17° for chitosan and alumina-chitosan nano-composite. The characterization of the products confirmed that the synthesis of chitosan and alumina-chitosan nano-composiote was effective.

Keywords: *Rhynchophorus phoenicis*, SEM, FTIR, Chitosan, XRD

INTRODUCTION

Rhynchophorus phoenicis, commonly called African Palm Weevil, is a species of beetles of the Curculionidae family. *Rhynchophorus phoenicis* can reach a body stretch of 25mm. It is considered a serious pest in palm plantations, particularly damaging young palms, mainly *Cocos nucifera*, *Metroxylon sagu*, *Raphia species*, *Elaeis guineensis* and *Phoenix dactylifera*. The African palm weevil has a complete life cycle with an egg, larva, pupa,

and adult stage. The adults lay eggs in wounds in the stems of dying or damaged parts of palms. After hatching, the weevil larvae excavate tunnels in the trunk and feed on the shoot and young leaves, frequently bringing about the ruin of the host plants. Cultural importance of the palm weevil is evident due to larvae being harvested and eaten (Ekpo and Onigbinde, 2005). This specie, which is spread all through the tropical regions of Africa where it is regarded as a pest because of its infestation of palm (Temitope, 2013), contains chitin.



Plate 1 *Rhynchophorus phoenicis* (African Palm Weevil)

Chitin is a hard, rigid, white, nitrogenous polysaccharide seen in the inner structure of invertebrates and in the exoskeletons. After cellulose, chitin is judged as the next most plentiful polysaccharide on earth with a making of approximately 1010-1012 Tons (Robert, 1992). Chitin is a homopolymer of 2-acetamido-2-deoxy-D-glucose (N-acetylglucosamine) residue linked by β -(1-4) bonds (Wang *et al.*, 2006).

Chitin is often considered as a derivative of a cellulose having both polysaccharide as the functional group but has acetamide groups ($-\text{NHCOCH}_3$) at the C-2 position (Pradip *et al.*, 2004). Naturally, there are three types of chitin that is different in structures, which are α -chitin, β -chitin and γ -chitin. α -chitin being the most plentiful has a tightly compacted orthorhombic cell made by alternated sheets of antiparallel chains (Minke and Blackwell, 1978); β -chitin having a monoclinic unit cell with polysaccharide chains attaching in a similar pattern (Gardner and Blackwell, 1975); γ -chitin is a mixture of β and α structure instead of a third polymorph (Robert, 1992). The formation of chitin is solid and bars it to dissolve in many solvent, hence, the need for chitin to be converted into chitosan (Peter, 1995).

Chitosan is one of the end products of chitin. Differed from chitin, chitosan are dissolvable in most solvent particularly acidic solvents which allow it to act as a cationic polyelectrolyte. Not long ago, chitosan has become more desirable than chitin as it is better in solution process. Chitosan comprises attributes as ordinary biopolymers such as biodegradability, non-toxicity and biocompatibility whereas it is exceptional owing to some attributes such as absorption and chelation properties, antimicrobial activity and film forming ability (Kumar, 2000). Additionally, its great formability enable it to be changed into powders, films, fibers, beads, coating, and solution which permit it to diverse its value (Kumar, 2000; Al Sagheer *et al.*, 2009). Usually, chitosan is a cationic polysaccharide owing to deacetylation of chitin with a straight chain structure comprising β -(1,4)-linked 2-acetamino-2-deoxy- β -D-glucopyranose with 2-amino-2-deoxy- β -D-glucopyranose (Marthur and Narang, 1990), thus a homopolymer of glucosamine and N-acetylglucosamine. Chitosan and chitin are carbohydrate gotten in nature from polymers which are seen in the exoskeleton of crustaceans (Shahidi and Abuzaytoun, 2005). Fungi's cell wall and insect's wing are as well stated to comprise

chitin (Tharanathan and Kittur, 2003). Chitosan and chitin are biopolymers that have outstanding attributes in biocompatibility, absorption, non-toxicity and biodegradability. Chitosan and chitin includes 6.9 %wt nitrogen in its structure and this acts as a chelating agent (Hudson and Smith, 1998). Chelating agent is the expression for organic compound with the capacity to carry out chelation. Moreso, chelation is explained as the capacity of the molecule or ion to combine with metal ion. The procedure encompassed the creation of two or more separate coordinate bond between a polydentate ligand and a central atom. This chelate effect portrayed the improved affinity of the chelating ligand on metal ions. Chitosan and chitin are both excellent chelating agents with the possession of these ligands.

Chitosan has been synthesized using different sea animals like shrimp shells using different methods (Mudit-Mishra *et al.*, 2013; Divya *et al.*, 2014; Patria 2013; Arafat *et al.* 2015), prawn shells (Musarrat *et al.*, 2013; Nessa *et al.*, 2010)

The aim of this study is to make relevant contributions involving the synthesis of alumina-chitosan nanocomposite and compare the characteristics of synthesized chitosan with the alumina-chitosan nanocomposites.

MATERIALS AND METHODS

Collection and Preparation of Samples

Rhynchophorus phoenicis were collected from palm trees at Omuoko community in Aluu, Ikwerre Local Government Area, Rivers state, Nigeria, and identified at the Department of Animal and Environmental Biology, University of Port Harcourt, Rivers State, Nigeria. The samples were

cleaned of adhering dirt and soft tissues, washed well with distilled water and kept in the oven at 50°C for two days. After drying, the dried samples were ground and sieved.

Demineralization

A 1000 mL beaker glass containing 650 mL of 1 M HCl solution was added 65g hard tissues of *Rhynchophorus phoenicis*. With a magnetic stirrer at room temperature for 3 hours, the mixture was stirred and then filtered with Whatman filter paper while constantly rinsed with distilled water until neutrality was achieved. The residue was kept in an oven at 65°C until dry to steady weight (Mohadi *et al.*, 2015).

Deproteinisation

The residue was put into a 1000 mL glass beaker and added 650 mL of 1 M NaOH solution. The mixture was stirred and heated for 1 hour on a hotplate at 60°C and then sieved with filter paper. The residue were washed with distilled water until the pH was neutral, and then put in an oven at 65°C until dry to stable weight. The residue gotten at this step is chitin. (Mohadi *et al.*, 2015).

Deacetylation

Deacetylation of chitin gives chitosan. The chitin was put into a glass beaker containing 50% NaOH solution at a ratio of 10:1 (w/v) between NaOH solution and the isolated chitin. The mixture was stirred and heated for 2 hours on a hotplate at 110°C. The mixture was filtered and the residue was washed with de-ionized water until the chitosan was neutral. Chitosan was put in an oven at 65°C until it was dry to steady weight (Mohadi *et al.*, 2015).

Synthesis of Alumina-chitosan nanocomposite

120 mL of 10 % oxalic acid was added to 6 g of chitosan and then heated at 55°C until it formed a gel. Then, 120 mL distilled water was added to the gel solution, and heated for 20 minutes at 45°C. Next, 12g of Al₂O₃ was added to the solution and stirred for 240 minutes at 250 rpm and left for 2 hours. The precipitate was filtered, cleaned and dried in an oven for 5 hours at 55°C (Fatma *et al.*, 2019).

Characterisation

The alumina-chitosan nanocomposites were characterized using the following instruments:

FTIR-8400S Fourier Transform Infrared Spectrometer between 4000 and 600 cm⁻¹ was employed for the FTIR spectra of chitosan alumina nanocomposite and chitosan.

XRD measurements for the chitosan alumina nanocomposite and chitosan were done by ARL X'TRA X-ray Diffractometer.

Pro-X Scanning Electron Microscope was employed to ascertain the morphological description of the chitosan alumina nanocomposite and chitosan.

RESULTS AND DISCUSSION

Chitosan and alumina-chitosan nanocomposites were characterized with the help of standard instruments.

Table 1: FT-IR Spectra Analysis for Chitosan

S/No	Wave Number (cm ⁻¹)	Intensity	Bond	Functional Group
1.	802.41	Strong	C-H bending	1,4-disubstituted
2.	925.86	Strong	C=C bending	Alkene
3.	1041.6	Strong	CO-O-CO stretching	Anhydride
4.	1303.92	Strong	C-N stretching	Aromatic amine
5.	1527.67	Strong	N-O stretching	Nitro compound
6.	1681.98	Strong	C=O stretching	Tertiary amide
7.	1790	Strong	C=O stretching	Conjugate acid halide
8.	1967.46	Medium	C=C=C stretching	Allene
9.	2129.48	Weak	C=C stretching	Alkyne
10.	2337.8	Strong	O=C=O stretching	Carbon dioxide
11.	2453.54	Weak	S-H stretching	Thiol
12.	2615.56	Weak	S-H stretching	Thiol
13.	2739.01	Weak, broad	O-H stretching	Alcohol
14.	2939.61	Medium	C-H stretching	Alkane
15.	3225.09	Medium	N-H stretching	Secondary amines
16.	3286.81	Medium	N-H stretching	Secondary amines
17.	3402.54	Medium	N-H stretching	Aliphatic primary amine
18.	3525.99	Medium	O-H stretching	Alcohol (free)
19.	3634.01	Medium, sharp	O-H stretching	Alcohol (free)
20.	3688.02	Medium, sharp	O-H stretching	Alcohol (free)

21.	3842.33	Medium, sharp	O-H stretching	Alcohol (free)
22.	3950.35	Medium, sharp	O-H stretching	Alcohol (free)

Chitosan is a biopolymer that encompasses many active binding spots. Fourier transform infrared spectroscopy is a well-known analytical technique that can give information on the nature and the content of existing functional and structural groups and it gives information by frequencies, intensities and bonding properties, and can consequently be applied to recognize species (Bhargava et al., 2003). The chemical composition and the bonding arrangement of constituents in a homopolymer, copolymer, polymer composite and polymeric materials in general can be obtained using Infra-red spectroscopy (Bhargava et al., 2003). FTIR range of the chitosan is displayed in figure 1. The broad band at 3842.33 cm^{-1} shows the existence of OH stretching vibrations. The point at 3402.54 cm^{-1} shows the existence of -NH stretching band and the peak around 3286.81 cm^{-1} and 3225.09 cm^{-1} shows the occurrence of NH bending. The spectra at 2939.61 cm^{-1} displays the vibration of methylene C-H bonding while the sharp

point at 2337.8 cm^{-1} displays the occurrence of O=C=O stretching. The spectra at around 1527.67 cm^{-1} came from C-N stretching. The point at 1303.92 cm^{-1} displays the occurrence of C-N stretching band. The stretch at 1041.6 cm^{-1} shows the occurrence of CO stretching vibration in band CO-O-CO.

Teli and Sheikh (2012) investigated the FT-IR spectra of chitosan extracted from shrimp shells. In the studies, chitosan absorption band features bending vibration of NH from R-NH₂ was observed at 1620.1 cm^{-1} indicating increase degree of deacetylation while C-H was displayed with stretching vibration of 2916.1 cm^{-1} , 2858.3 cm^{-1} and bending vibration of 1415.7 cm^{-1} , 1375.2 cm^{-1} . The result was compared with commercial chitosan and a significant degree of similarities was observed. The FT-IR spectra of this study are similar to the studies reported by Bensaha and kara (2015), Mohammad *et al.* (2013).

Table 2 : Reference Bands, Waves Number and Their Advantages and Disadvantages.

[Adapted from Kasaai (2008)]

Absorption Band	Wave number (cm-1)	Advantages	Disadvantages
O-H stretching	3450	OH has highly intense absorption band	(1) O-H of water molecule appears in this region; (2) O-H groups involve with intra- and intermolecular hydrogen bonds and result in a broad peak; (3) N-H stretching band appear around 3300 cm^{-1} and creates an

C-H stretching	2870	The intensity of peak is significant; the band does not involve in hydrogen bonds; and water does not create any interference peak	interference peak and its intensity changes with the DA The position of C-H stretching corresponding to N-acetyl groups changes with the DA
CH₂ bending	1420		Shape and intensity of the peak change with changing the crystallinity of chitosan samples through rearrangement of hydrogen bonds at position of primary OH-groups
C-O stretching	1030		Several absorption bands appear
C-O stretching	1070		in this region; and the peak is
C-O stretching of glycoside linkage	897		not clearly separated, and its
Glycoside linkage/ C-OC bridge (asymmetric CO-stretching)	1160		intensity is weak

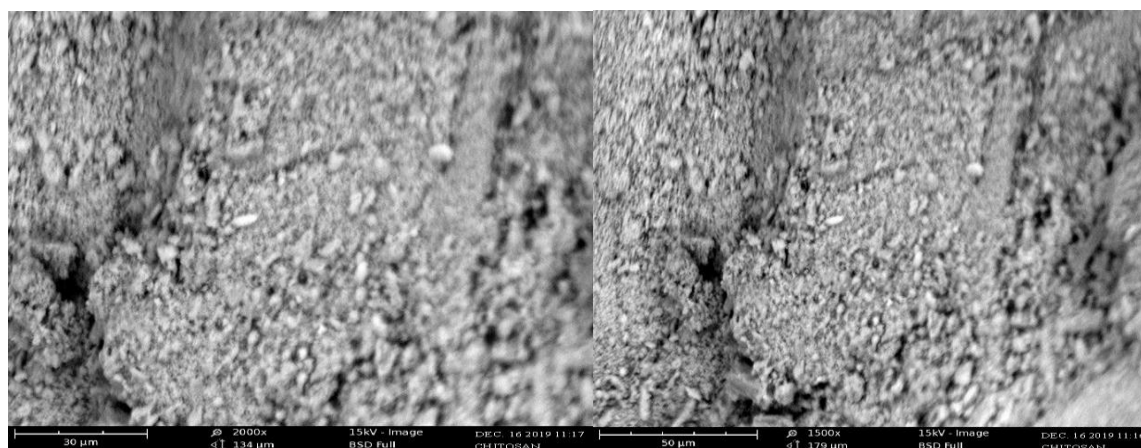
Table 2: FT-IR Spectra Analysis for Alumina-chitosan Nanocomposite

S/No	Wave Number (cm⁻¹)	Intensity	Bond	Functional Group
1.	748.41	Strong	C-H bending	Monosubstituted
2.	910.43	None	None	None
3.	1018.45	Strong	C=C bending	Alkene
4.	1080.17	Strong	C-O stretching	Primary alcohol
5.	1265.35	Strong	C-N stretching	Aromatic amine
6.	1535.39	Strong	N-O stretching	Nitro compound
7.	1681.98	Strong	C=O stretching	Tertiary amide
8.	1982.89	Medium	C=C=C stretching	Allene
9.	2144.91	Strong	N=C=N stretching	Carbodiimide
10.	2337.8	Strong	O=C=O stretching	Carbon dioxide
11.	2445.82	Weak	S-H stretching	Thiol
12.	2530.69	Weak	S-H stretching	Thiol
13.	2615.56	Weak	S-H stretching	Thiol

14.	2746.73	Medium	C-H stretching	Aldehyde
15.	2931.9	Medium	C-H stretching	Aldehyde
16.	3232.8	Strong, sharp	C-H stretching	Alkyne
17.	3363.97	Medium	N-H stretching	Aliphatic primary amine
18.	3495.13	Strong, broad	N-H stretching	Primary amide
19.	3626.29	Medium, sharp	O-H stretching	Alcohol (free)
20.	3742.03	Medium, sharp	O-H stretching	Alcohol (free)
21.	3826.9	Medium, sharp	O-H stretching	Alcohol (free)
22.	3981.21	Medium, sharp	O-H stretching	Alcohol (free)

FTIR spectrum of the alumina-chitosan nanocomposite is presented in figure 2. The bands at 3841.21cm^{-1} , 3826.9cm^{-1} , 3742.03cm^{-1} and 3626.29cm^{-1} prove the occurrence of OH stretching vibrations. The stretch at 3495.13cm^{-1} and 3363.97cm^{-1} show the occurrence of N-H stretching band. The sharp stretch at 2931.9cm^{-1} represents the vibration of methylene C-H bonding while the sharp stretch at 2337.8cm^{-1} indicates the occurrence of O=C=O stretching. The spectra at around 1265.35cm^{-1} came from C-N stretching. The peak present at 1080.17cm^{-1} confirms the occurrence of C-O stretching band. The intensity of peaks slightly decreased when compared with Peaks obtained for chitosan. The relative peaks changed because of blending with alumina and metal-Chitosan complex formation between metal ion and hydroxyl group of Chitosan (Holopainen et al., 1998; Zhang and Yin (1999))

Scanning Electron Microscope (SEM)



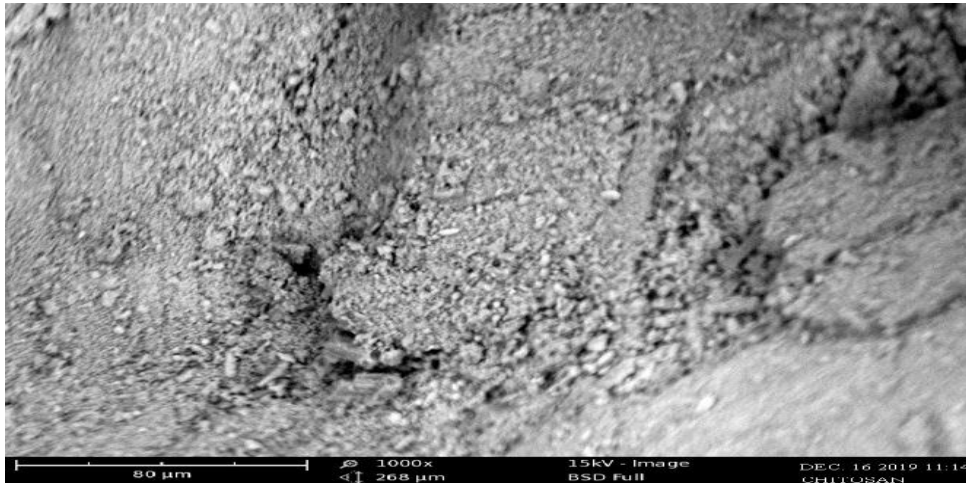


Plate 1: SEM Micrograph of Chitosan

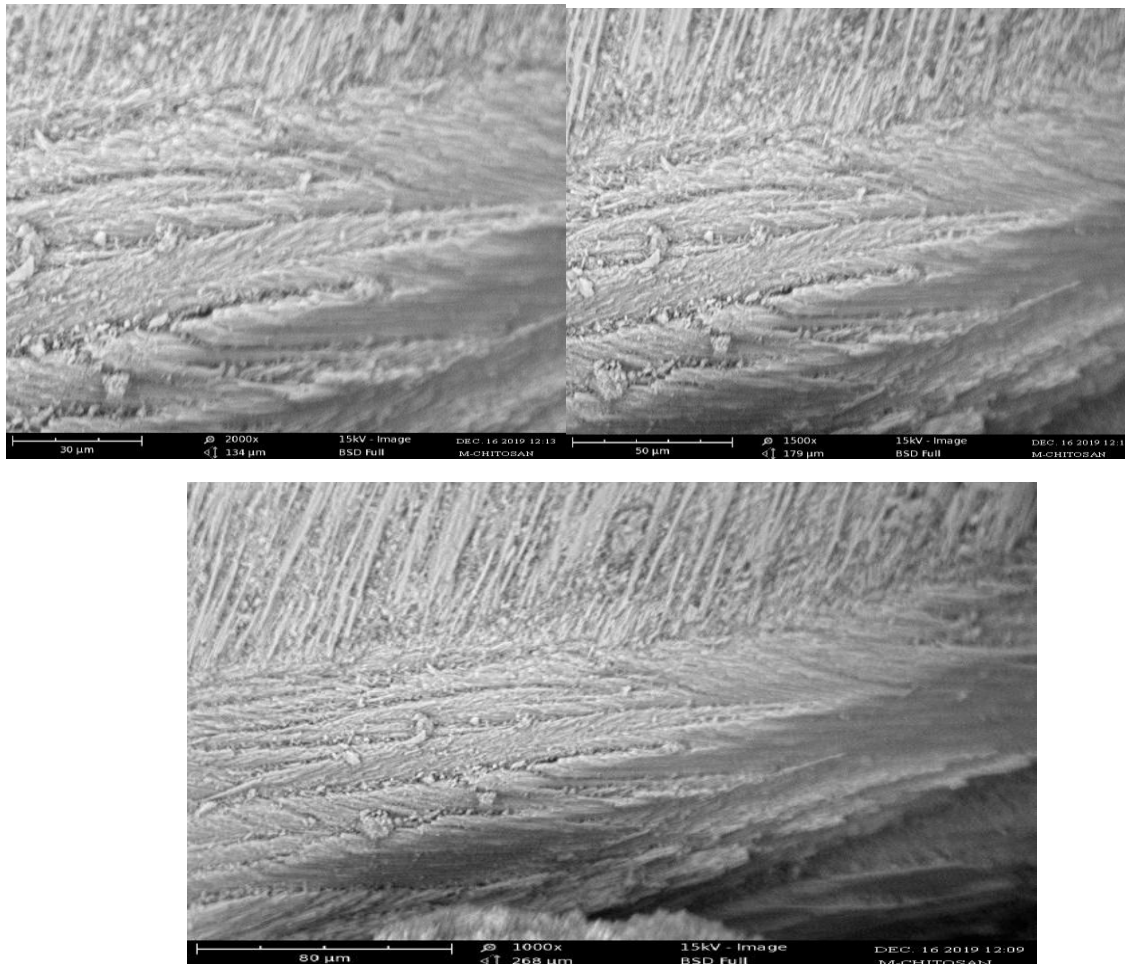


Plate 2: SEM Micrograph of Alumina-chitosan Nanocomposite

Plate 1 and 2 displays the SEM micrograph of the chitosan and alumina-chitosan nanocomposite. From plate 1, it was revealed that the chitosan has large (crystalline) particles that are regular with paltry pores. Plate 2 revealed that the alumina-chitosan nanocomposite has fairly small particles and porous surface with significant pores. The results obtained in the SEM micrograph are similar to Zhang et al. (2012) and Islam et al. (2011).

X-ray Diffraction

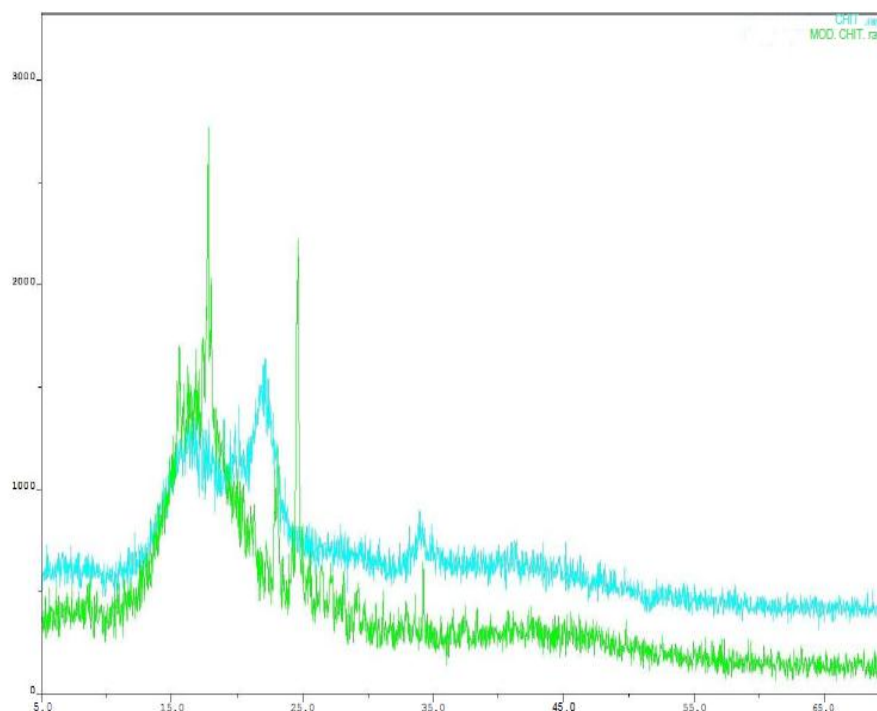


Figure 3: Combined XRD Pattern of Chitosan and Alumina-chitosan Nanocomposite

Figure 3 presents the XRD outline of the alumina-chitosan nanocomposite and chitosan. XRD study investigates the crystalline behaviour of the samples. In the diffractogram, chitosan gives broad stretch at 22° and 16° whereas the alumina-chitosan nanocomposite gives distinct stretch at 25° and 17° . This symbolised semi-crystalline chitosan. The X-ray graph shows that the chemically treated chitosan peaks were more intense than untreated chitosan. This is similar to Yen et al. (2009), Tang et al.(2006), Islam et al.(2011). The dissimilarity and alterations between the SEM morphology, XRD pattern and FTIR spectrum of the alumina-chitosan nanocomposite and chitosan confirms that the production of alumina chitosan nanocomposite and chitosan was effective.

CONCLUSION

Chitosan and alumina chitosan composite have been synthesized from hard shell of *Rhynchophorus phoenicis* using standard methods. The products synthesized were characterised using XRD, SEM and FTIR. The characterization revealed the crystalline behaviour, types of functional groups and the sizes of the particles of the products synthesized. The products were verified as chitosan by its FT-IR identification bands matching with chitosan of other study.

REFERENCES

- Al Sagheer, F. A., Al-Sughayer, M. A., Muslim, S. and Elsabee, M. Z. (2009). Extraction and characterization of chitin and chitosan from marine sources in Arabian Gulf. *Carbohydrate Polymers* 77(1), pp. 410-419.
- Arafat A., Samad S. A., Masum S. Md., and Moniruzzaman M. (2015). Preparation

- and characterization of chitosan from shrimp shell waste. *International Journal of Scientific & Engineering Research*, Volume 6, Issue 5.
- Bensaha Sofiane and Kara Slimane Sofia (2015), Biosorption of heavy metals by chitin and the chitosan. *Der Pharma Chemica*, 7(5):54-63.
- Bhargava, R., Wang, S. & Koenig, J.L. (2003). FTIR Microspectroscopy of polymeric systems, *Avances in Polymer Science*, 163; 137 – 191.
- Divya K., Rebello S. and Jisha M. S. (2014). A Simple and Effective Method for Extraction of High Purity Chitosan from Shrimp Shell Waste. *Proc. of the Intl. Conf. on Advances In Applied Science and Environmental Engineering – ASEE.*, ISBN: 978-1-63248-004-0 doi: 10.15224/ 978-1-63248-004-0-93.
- Ekpo, K. and Onigbinde, A. (2005). Nutritional potentials of the larva of *Rhynchophorus phoenicis* (F). *Pakistan Journal of Nutrition* 4: 287–290.
- Fatma, Yuliasari N., Riyanti F., Hariani P. L., and Nurbaiti B. (2019). Synthesis of chitosan/alumina composite by sol gel method for adsorption of procion blue MX-R dye from wastewater songket industry. *Journal of Physics: Conf. Series* 1282 (2019) 012080.
- Gardner, K. H. & Blackwell, J. 1975. Refinement of the structure of Beta-Chitin *Biopolymers*, 14, pp. 1581-1595.
- Goldstein, J. 2003. Scanning electron microscopy and x-ray microanalysis. Kluwer Academic: Plenum Publishers.
- Holopainen, T., Alvila J. Rainio, T. and Pakkanen, T. (1998). IR spectroscopy as a quantitative and predictive analysis method of phenol-formaldehyde resol resins. *J. Appl. Polym. Sci.* 69; 2175 – 2185.
- Hudson, S. M. & Smith, C. 1998. Polysaccharide: chitin and chitosan: chemistry and technology of their use as structural material. *Biopolymers from renewable resource*. New York: Springer-Verlag.
- Kasaai, M. R. 2008. A Review of several reported procedures to determine the degree of N-acetylation for chitin and chitosan using infrared spectroscopy. *Carbohydrate Polymers*, 71, pp. 497-508.
- Kumar, M. N. V. R. 2000. A review of chitin and chitosan applications. *Reactive and Functional Polymer*, 46 (1), pp. 1-27.
- Islam, M. M., Masum, S. M., Molla, M. A. I., Rahman, M. M., Shaikh, A. A. & Roy, S. K. 2011. Preparation of Chitosan from Shrimp Shell and Investigation of Its Properties. *Intenational Journal of Basic & Applied Sciences* 11 (1), pp.116-130.
- Marthur, N. and Narang, C. (1990). Chitin and Chitosan, Versatile Polysaccharides From Marine Animals. *Journal of Chemical Education*, 67, pp. 938-42.
- Minke, R. & Blackwell, J. 1978. The Structural of Alpha-Chitin *Journal of Molecular Biology*, 120, pp. 167-181.
- Mohadi R., Kurniawan C., Yuliasari N., Hidayati N. and Aldes Lesbani (2015). Synthesis of Nanocomposite Chitosan-Tio2 and its Application as Photodegradation Agent of Methilen Blue in Aqueous Medium. *Progress on Chemistry and Application of Chitin and its Derivatives*, Volume xx, doi: 10.15259/PCACD.20.21.

- Mohammed, M. H., Williams, P. A. & Tverezovskaya, O. 2013. Extraction of chitin from prawn shells and conversion to low molecular mass chitosan. *Food Hydrocolloids*, 31, pp. 166-171.
- Mudit-Mishra V. M., Paliwal J. S., Singh S. Kr., Selvarajan E., Suganthi V. and Subathra Devi C. (2013). Studies on heavy metal removal efficiency and antibacterial activity of chitosan prepared from shrimp shell waste. *3 Biotech* DOI 10.1007/s13205-013-0140-6.
- Musarrat H. M., Peter A. W., and Olga T. (2013). Extraction of chitin from prawn shells and conversion to low molecular mass chitosan. *Food Hydrocolloids* 31:166-171.
- Nessa F., Masum Shah Md., Asaduzzaman M., Roy S. K., Hossaina M. M. and Jahan M. S. (2010). A Process for the Preparation of Chitin and Chitosan from Prawn Shell Waste. *Bangladesh Journal of Scientific and Industrial Research*, 45(4), 323-330, 2010.
- Patria A. (2013). Production and characterization of Chitosan from shrimp shells waste. *AAFL Bioflux*, volume 6, Issue 4.
- Peter, M. (1995). Applications and environmental aspects of chitin and chitosan. *Journal of Macromolecular Science, Part A: Pure Applied Chemistry*, A32 (4), pp. 629-40.
- Pradip, K. D., Joydeep, D. and Tripathi, V. S. (2004). Chitin and chitosan: Chemistry, properties and applications. *Journal of Science and Industrial Research*, 63, pp. 20-31.
- Robert, G. A. F. (1992). *Chitin Chemistry (1st ed.)*, London, Macmillan.
- Shahidi, F. and Abuzaytoun, R. (2005). Chitin, Chitosan, and Co-products: Chemistry, Production, Applications, and Health Effects. *Advance Food Nutrition Research*, 49, pp. 93-135.
- Teli, M. D. & Sheikh, J. 2012. Extraction of chitosan from shrimp shells waste and application in antibacterial finishing of bamboo rayon. *International Journal of Biological Macromolecules*, 50, pp. 1195-1200.
- Temitope, O. O. (2013). Morphology and histology of the alimentary tract of adult palm weevil, *Rhynchophorus phoenicis* Fabricius (Coleoptera: Curculionidae). *Journal of Developmental Biology and Tissue Engineering* 5: 13–17.
- Tharanathan, R. N. and Kittur, F. S. (2003). Chitin-The Undisputed Biomolecule of Great Potential. *Critical Review on Food Science and Nutrition*, 43, pp. 61-87.
- Trung, T. S., Thein-Han, W. W., Qui, N. T., Ng, C.-H. & Stevens, W. F. 2006. Functional characteristics of shrimp chitosan and its membranes as affected by the degree of deacetylation. *Bioresource Technology*, 97 (4), pp. 659-663.
- Wang, S. L., Lin, T. Y., Yen, Y. H., Liao, H. F. and Chen, Y. C. (2006). Bioconversion of Shellfish Chitin Wastes for the Production of *Bacillus Subtilis* W-118 chitinase. *Carbohydrate Research*, 341(15), 2507-15.
- Yen, M.-T., Yang, J.-H. & Mau, J.-L. 2009. Physicochemical characterization of chitin and chitosan from crab shells. *Carbohydrate Polymers*, 75, pp. 15-21
- Zhang, H., Jin, Y., Deng, Y., Wang, D. & Zhao, Y. 2012. Production of chitin

from shrimp shell powders using *Serratia marcescens* B742 and *Lactobacillus plantarum* ATCC 8014 successive two-step fermentation. *Carbohydrate Research*, 362 (1), pp. 13-20.

Zhang L.M. and Yin, D.Y. (1999). Novel modified liganosulfonate as drilling mud thinner without environmental concern. *J. Appl. Polym. Sci.* 74; 1662-1668.